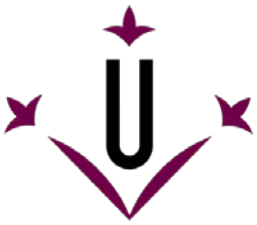

Universitat de Lleida

Experimental performance of a Fresnel-transmission PVT concentrator for building-façade integration

D. Chemisana[1,*], J.I. Rosell[1], A. Riverola[1], Chr. Lamnatou[1]

[1]Applied Physics Section of the Environmental Science Department, University of Lleida, Jaume II 69, 25001, Lleida, Spain.

*Correspondence e-mail: daniel.chemisana@macs.udl.cat

Abstract

A building-façade integrated concentrating photovoltaic-thermal system has been designed, constructed and experimentally characterised. Comparative performances with a non-concentration reference unit have been conducted to analyse the differential outputs. The concentrating system consists of double-side reflective strips which concentrate the incident beam towards a static photovoltaic-thermal receiver. The reflectors are placed vertically at the façade and track the sun by rotating axially. The concentrating reflector outperforms the reference one in both, thermal and electrical power. The thermal output of the concentration module almost doubles the reference one and the electrical power registered is more than 4.5 times in the case of the concentrating configuration.

Keywords: Building integration; Solar concentration; Photovoltaic-Thermal (PVT) collectors; Concentrating Photovoltaic (CPV)

1 Introduction

Energy consumption in the building sector represents 40% of the total energy consumed in the European Union. The European Commission, in order to decrease energy consumption, defined (considering buildings as a priority) the directive which states the “20-20-20” objectives: greenhouse gas emissions reductions (20%), the share of renewable energy (20%) and improvements in energy efficiency (20%) [1]. In this regard, Building Integrated Solar (BIS) systems are a technology which perfectly addresses the objectives defined by the European Union.

Among BIS technologies, Building-Integrated Concentrating Photovoltaic (BICPV) systems present some characteristics that could qualify them as an attractive and feasible configuration to be incorporated in buildings. The reduction of cell area which is replaced by cheaper and more environmentally friendly materials can lead to more cost-efficient systems from both, economical and environmental aspects [2]. However, it is necessary to mention that the irradiance captured by the concentrating systems is, in general, lower than for a standard PV module due to optical losses and the diffuse irradiance fraction which is not collected. The diffuse irradiance portion used changes with the concentration ratio: for low-concentration systems a high percentage of diffuse light is useful whilst for high-concentration devices only the direct irradiance converges onto the PVs. The concentrating element plays a dual function by balancing the light that passes into the interior space and the light that converges onto the PVs. Several configurations of BIPV systems can be found in the literature, either for installing at the roof or at the façade [3-12]. Most of them are designed to be static with low concentration ratios, but others increase the concentration ratio by incorporating a solar tracking system. Medium and high-concentration systems offer high reduction in

PV cells usage and therefore, the highest the concentration the best the cost-effectiveness ratio. High-concentration systems use PV cells which achieve electrical efficiencies above 40% and the cell surface is minimised, which reduces the impact regarding the economical and environmental associated costs of the system [13-15]. Nevertheless, high-concentration technologies require a very accurate two-axis tracking system and movement of the whole CPV system is produced. Medium-concentration technologies (10-100 suns) present some possible advantages with respect to low- and high-concentration devices. From one side, the concentration is higher than in static artefacts and this means a reduction in cells quantity with its consequent impact on cost. From the other side, medium concentration systems allow for single-axis tracking which simplifies the mechanics and the control associated [16-19].

On the contrary, when increasing the concentration ratio the percentage which is not converted into electricity becomes much higher in absolute terms. This could cause PV overheating and thus, problems related with efficiency reduction, stress of materials, etc arise. A strategy to profit the removal heat which negatively influences system performance is to use a hybrid Photovoltaic-Thermal (PVT) receptor. PVT module controls PV temperature while simultaneously produces thermal energy. Hybrid collectors integrated onto the building could be an interesting option as both energies, thermal and electrical, could be directly used [20-24].

With respect to studies about the specific type of BICPVT systems, Chemisana et al. [25] characterised a PVT module for applications with Fresnel linear concentrators. The optimized optical concentrator referred to linear focal area, homogeneous illumination conditions and variable concentration ratios from 7x to 10x. The optical unit was based on a stationary wide angle optical concentrator which

transmitted the input radiation into a small moving focal area, which in turn was tracked by the solar absorber [25]. Xu et al. [26] developed a low-concentrating PVT integrated heat pump system with both electricity and heat outputs. Fixed truncated parabolic concentrators with geometrical concentration ratio of 2.44x were adopted [26]. Moreover, a roof-integrated concentration solar system for a self-sustainable Mediterranean villa, the Astonyshine house, was investigated [27]. The Astonishine house was designed in such a way that a great part of its electrical power and hot water needs are satisfied by Solar F-Light modules mounted on the house roof. The Solar F-Light is a parabolic linear trough with single-axis tracking and 20x optical concentration factor. Li et al. [27] proposed a system with an air-gap-lens-walled compound parabolic concentrator incorporated with PVT, having a geometrical concentration ratio of 2.4x and static concentrator.

Based on the previous paragraphs, it can be seen that in the literature there are few studies about BICPVT while most of these works are about low-concentration configurations. Given the fact that medium-concentration PVT systems can offer multiple advantages in the frame of BI applications, in the present work a medium-concentration system for façade building-integration has been constructed and experimentally characterised. The prototype consists of a Fresnel-reflector concentrator which delivers solar irradiance onto a PVT module. The concentrator was sought to be simple from both points of view: materials employed and associated tracking. The research covers the mechanical design of the concentrator, the construction of the whole system and its experimental characterisation. Firstly, section 2 describes the optical, mechanical and generation parts to later include the experimental set-up built to perform the monitoring (section 3). In section 4, results regarding optical, electrical and thermal performances are discussed to finally present the main conclusions in section 5.

2 System description

2.1 Optical system

The optical analysis of the present system is described in detail in ref. [17], where the optical design methodology is included and several configurations were theoretically analysed.

The most important parameters and characteristics involved in the optical design are briefly illustrated in figures 1a and 1b. Fig. 1a shows the parameters used in system design, for a configuration of 21 reflectors. Parameter f represents the focal length, the distance of the centre of rotation of the i^{th} reflector from the origin O is defined to be x_i and the angle subtended at the centre of the receiver by the reflector and the origin is α_i. The relation between them is: $\alpha_i = atan(x_i / f)$. θ_s is the angle of incidence of the solar radiation and the inclination of reflectors is defined as β_i. Both angles are related by $\beta_i = 0.5(\theta_s - \alpha_i)$ and the variation of β_i with respect to θ_s is 0.5 ($\partial\beta_i / \partial\theta_s = 0.5$). This means that once the initial position of the reflectors has been established, the relative movement required to achieve sun tracking is the same for all reflectors. This permits the use of a single linear driver, representing an important mechanical advantage. The receiver remains static while sun tracking is performed by the reflectors rotating simultaneously.

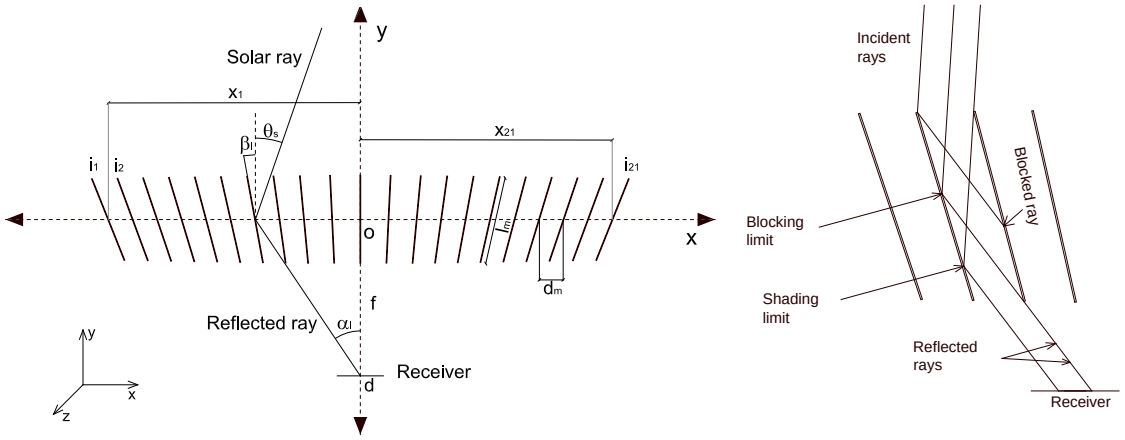

a) b)

Figure 1. a) Schematic showing parameters used in the mathematical model; b) shading and blocking effects.

Two phenomena are crucial in terms of system efficiency: blocking and shading. The positions of the upper and lower limits of the shaded and blocked rays are illustrated in figure 1b. The rays that fall on the mirror to the left of the shading limit are shaded and those that fall to the right of the blocking limit are blocked; therefore, optical efficiency decreases. These limits have been calculated by using a ray tracing algorithm. Once the algorithm converged for a selected set of parameters, an optimisation procedure for maximising the optical efficiency and the flux uniformity on the receiver, in a range of angles of incidence [-45º, 45º], was applied to obtain the best option for each studied configuration.

In the present investigation, from the optical theoretical results described in [17], the concentrating system has been constructed. It consists of 11 strips of double-side reflective material of 160 mm wide by 2000 mm long. The thickness of each reflector is 4 mm. The Numerical Aperture (NA) of the system is 0.5, with an entrance pupil of 800 mm by 2000 mm.

2.2 Photovoltaic-thermal module

The PVT module consists of 13 series connected crystalline silicon cells optimized for concentrating systems operating in a range from 10 to 20 suns (Fig. 2). The size of each cell is 3.5 cm by 4.8 cm. The cells (NaREC®) are attached to a water active heat dissipater with a special adhesive tape with high heat-transfer conductivity that is also resistant to extreme temperatures and an excellent electrical insulator (Chomerics Thermattach T404). The hybrid absorber is enclosed in an aluminium case with U cross-section made of copper where PV cells are placed (Fig. 2); the encapsulation of the collector is finished fixing one top glass cover of 77.5 mm wide by 600 mm long by 4 mm thick. From these dimensions it can be arranged the geometrical concentration ratio (ratio between the concentrator aperture area and receiver area), which takes a value of 16.67x with respect to the cell width and 10.32x with respect to the PVT module gross width.

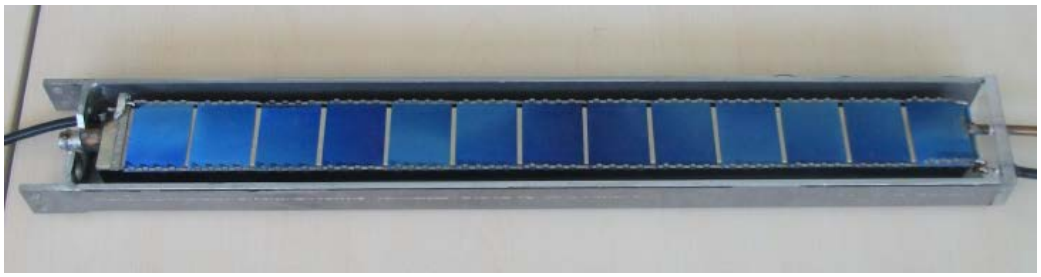

Figure 2. PVT module fabricated before the top glass fixing and detail of the module cross-section.

2.3 Mechanical structure

The 11 reflectors are fixed and placed vertically in a metallic framing structure. The inferior and superior profiles are drilled and prepared to hold the reflectors and at the same time to allow them rotating. The metallic frame constitutes the South façade of a testing-unit made of 4 cm wood white panes which was built to house all the sensors and instruments for the experimental campaign and to achieve more controlled testing conditions by minimising the wind effect, the ground temperature influence, albedo, etc.

In order to transform the rotational movement required to track the sun by the mirrors into a linear one, each reflector was attached mechanically onto a steel plate designed to have one point at the rotation centre of the reflector and another located with the corresponding angle for the specific reflector strip. In this manner, all reflectors are driven with the same actuator through the connecting rods fabricated (Figure 3).

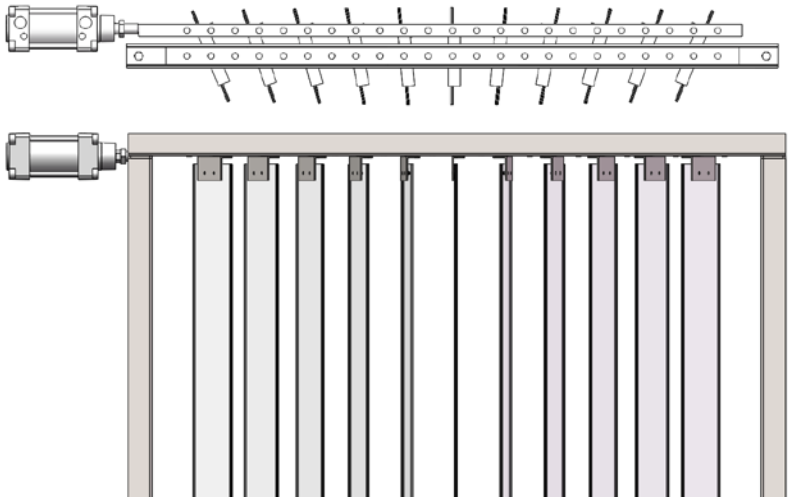

Figure 3. Detail of the mechanical system for tracking. Top and frontal view of the concentrating system.

As explained in 2.1, the angular rotation of the reflectors is equal in all of them, and at the same time is the half than the angular movement of the Sun. To transfer this relation, a very simple reduction gear (1:2) is used (Fig. 4). The tracking control is conducted by means of 2 photo resistances and a shading plate connected to an electronic circuit which in function of the current delivered from the resistors transfers a pulse to the actuator. In figure 4, a picture of the built prototype shows the tracking and control system. On the left it can be seen the control box, the driver with a limit switch sensor. The light sensor which tracks the sun through the photo resistances can be seen on the right of the image.

Figure 4. Detail of the implemented tracking system.

In this configuration, reflector strips rotate with respect to their vertical axis. It keeps tracking of the solar azimuth in its daily path. Its incorporation as an architectural element could replace a constructive element such as a vertical lattice arrangement. Receivers can be placed at the façade or in any location in order to facilitate the interconnection of different facilities.

3 Experimental testing set-up

The experiments were carried out at the Applied Energy Research Centre (CREA) at the University of Lleida (Spain), which is located in Lleida at latitude 41.36^{o}N and longitude 0.37^{o}E. Figure 5 shows the experimental installation during one of the tests. In the photograph, two modules, the reference and the concentrated one, can be seen. This configuration was adopted in order to perform differential assessment, taking as reference the module without concentrator. Also it can be observed the hydraulic circuit of both modules connected to the water tank. In Figure 6, a schematic of the monitoring system is depicted.

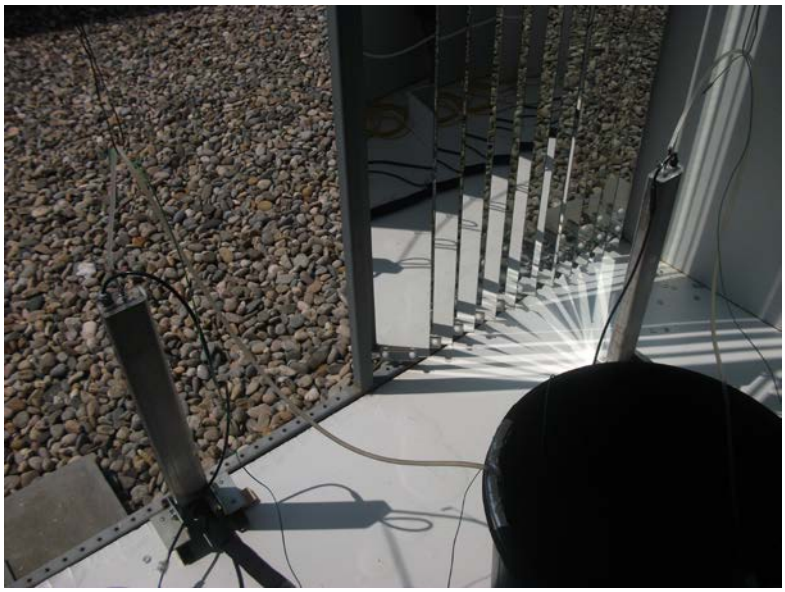

Figure 5. Experimental set-up during operation.

Differential performances were monitored according to the diagram which is shown in Fig. 6. The electrical parameters were measured by using two switching relay circuits to alternate short circuit and open circuit conditions every 30s. The short circuit currents were monitored through a Fluke i30s amperimetric clamp (accuracy ± 1 % of reading ± 2 mA) connected to a data acquisition (DAQ) system (datalogger Campbell

CR3000). Open circuit potential and relays were also collected and controlled respectively through the DAQ system. The thermal behavior of the systems was characterized by recording the inlet and outlet temperatures of the PVT modules by means of T-type thermocouples (accuracy ± 0.5ºC). In addition, a Kipp & Zonen CMP11 pyranometer (daily uncertainty < 2%) was positioned vertically at the wall at the same height than the modules. All the sensors were connected to the datalogger. The different input variables were measured every 1 s and their mean values were recorded every 5 s. For data processing and graphical representations, 30-second averaging was performed (in agreement with the switching time of relays).

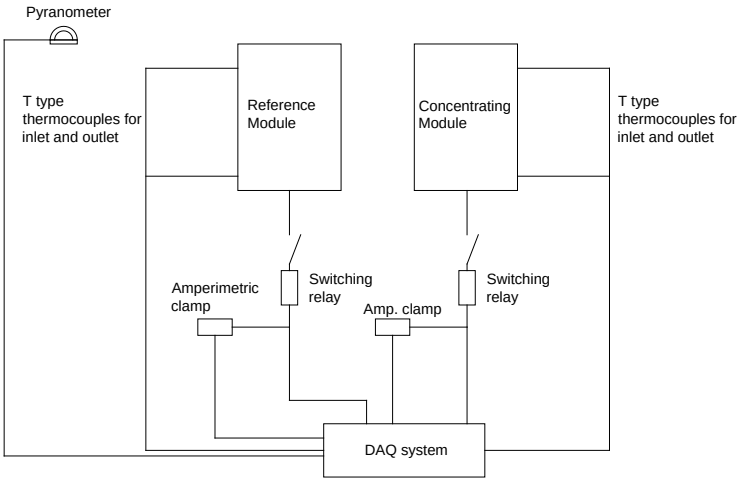

Figure 6. Schematic of the monitoring system.

3.1 Calibration of the PV modules

The PVT modules were fabricated manually and for this reason, even the components were the same, a previous analysis of both modules was necessary. For this purpose, a set of IV (current-potential) curves were collected employing the IV tracer PVPM 2540C to compare module performance under the same temperature and irradiance conditions. In Figure 7, the results of their calibration are illustrated.

As it can be noticed, PV modules present a small average relative difference in short circuit current of 4.2%. Even though this difference is very small, a normalization factor is accordingly adopted for the correction of the measured values during the experiments. With regard to the open circuit conditions, the potential difference between both is slightly higher than in the case of the short circuit current, taking a relative percentage value of 7.11%. As in the case of the current, a normalization factor is adopted for the correction of this difference.

In terms of the Fill Factor (FF), the average FF for the reference module is 0.79 whilst for the concentrating module the value was found to be 0.76. This value was considered to be constant for the calculation of the maximum power delivered by the modules, as maximum temperature variations of the PVs during the measurements daily campaign are about 15ºC-20ºC and concentration ratio is below 6 suns. These changes would affect the fill factor in a percentage less than 1% [29].

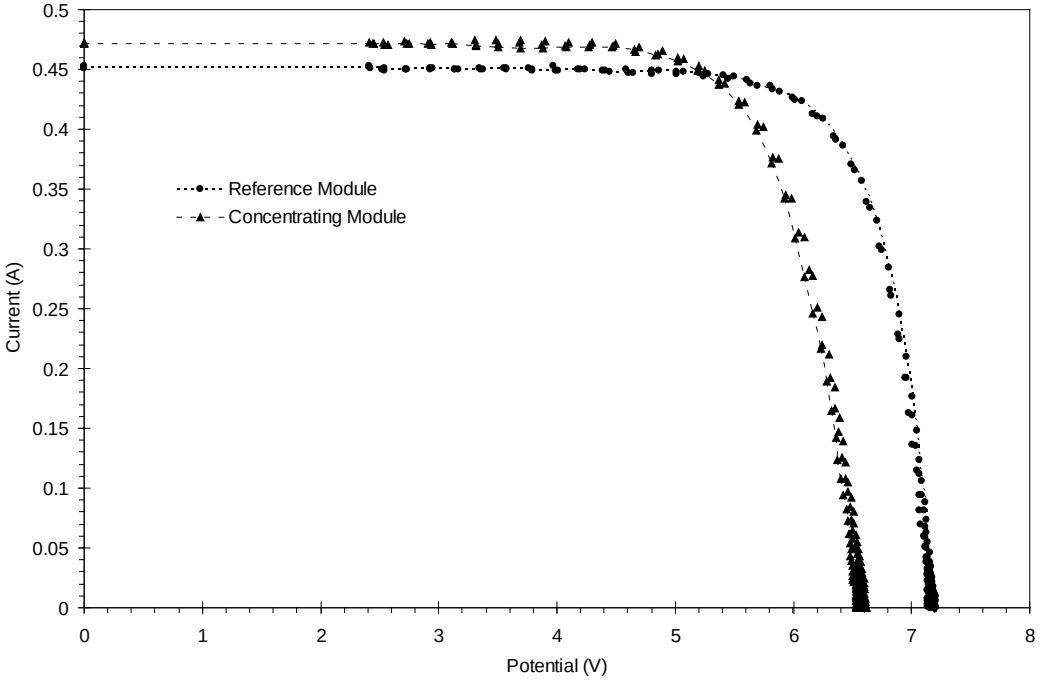

Figure 7. PV modules IV curves obtained under irradiances [948-952] W/m^2 and temperatures [38-41] °C.

4 Results

4.1 Optical efficiency

The optical efficiency was calculated from the electrical parameters measured. Since the short circuit current is proportional to the solar irradiance on the cell, the optical efficiency (η_o) can be determined by dividing the short circuit current of the concentrating module by the geometrical concentration (C_g) and the short circuit current of the reference module:

$$\eta_o = \frac{I_{sc,CPV}}{C_g \, I_{sc,PVref}} \tag{1}$$

For a clear sky day, the optical efficiency values achieve the pattern shown in Fig. 8.

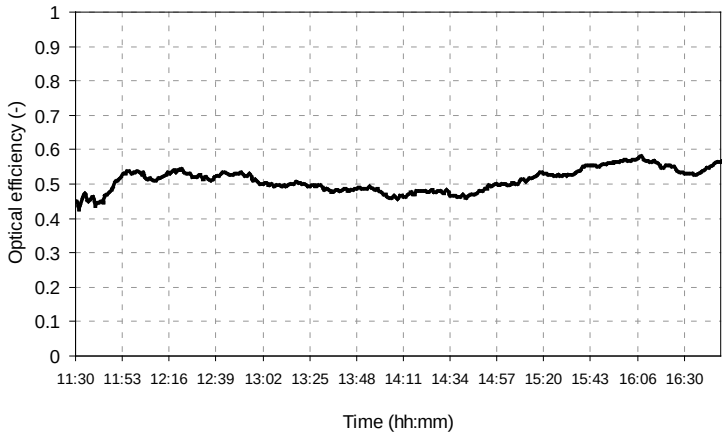

Figure 8. Daily temporal evolution of the concentrator optical efficiency. Date: 26/9/2014.

The mean optical efficiency achieved is 0.51. This value agrees very well with the equivalent calculated through simulation in [17], which was referred as Base System (BS) configuration. In this previous research, the authors found a daily efficiency

average value of 51.87 % for a range of angles of solar incidence from -45º to 45 (6-hour time period). It should be noted that the present efficiency is calculated for a 5-hour time period, which corresponds to the interval from -37.5º to 37.5º. For this narrower range of angles the simulated optical efficiency takes a value of 57.95%. The 7% difference observed from the experimental value to the simulated one is attributed to two factors: (1) a few tracking mismatch caused by the pulses delivered to the driver which, as it can be observed in Figs. 8 and 9, do not follow the sun continuously; (2) 90% average reflectance was considered in the simulation whilst the average reflectance of the reflector used was measured to be slightly lower (87%).

4.2 Electrical and thermal performance

The electrical performance of the system was characterized, as explained in section 3, by measuring the short circuit and open voltage conditions, as both are two key parameters to determine the effect of the solar concentration from the irradiance and temperature points of view.

In figure 9, the short circuit current and the open circuit potential for both, the CPV and reference modules, are represented jointly with the solar irradiance. As it is mentioned in the introduction, the diffuse irradiance fraction in the case of the CPV systems is not collected as in the case of the reference system because of the concentrator effect. Anyhow, in the present study, since the concentration ratio is low and in Lleida the diffuse fraction is usually quite low (around 12%), the differential performance due to this factor is low. In the case of a higher concentration system or for a location with higher diffuse irradiance fraction, divergences could affect more the comparison conducted.

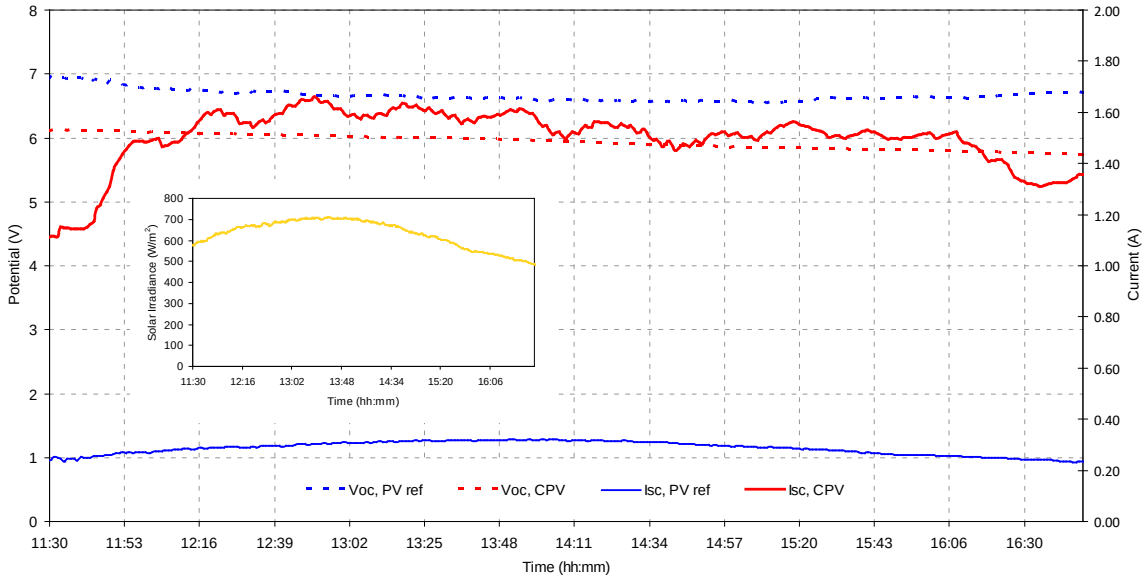

Figure 9. Irradiance, V_{oc} and I_{sc} profiles for the reference and the concentrating modules. Date: 26/9/2014.

The short circuit current of the reference module presents exactly the same profile than the irradiance curve, as expected. However, due to the action of the reflectors, apart that the current increases proportionally with the concentrated light, the CPV module is subject to local variations because the reflectors control actuates by pulses; thereby, the solar tracking suffers small mismatches. The open circuit potential, by contrast, reflects that the CPV module operates always worse than the reference module with a 10% difference in average. This fact is predictable since the concentrated irradiance that is not converted into electricity must be evacuated as heat, and as both modules are cooled with the same flow rate (3 l/h), the temperature of the CPV module is always higher. In Figure 10, this effect is illustrated. The inlet temperature for both modules is the same as the water tank from were the pump distributed the inflows is the same. The outlet flows are connected also to the tank in a closed-loop circuit. The temperatures average relative difference between the CPV and the reference modules is 11.3%.

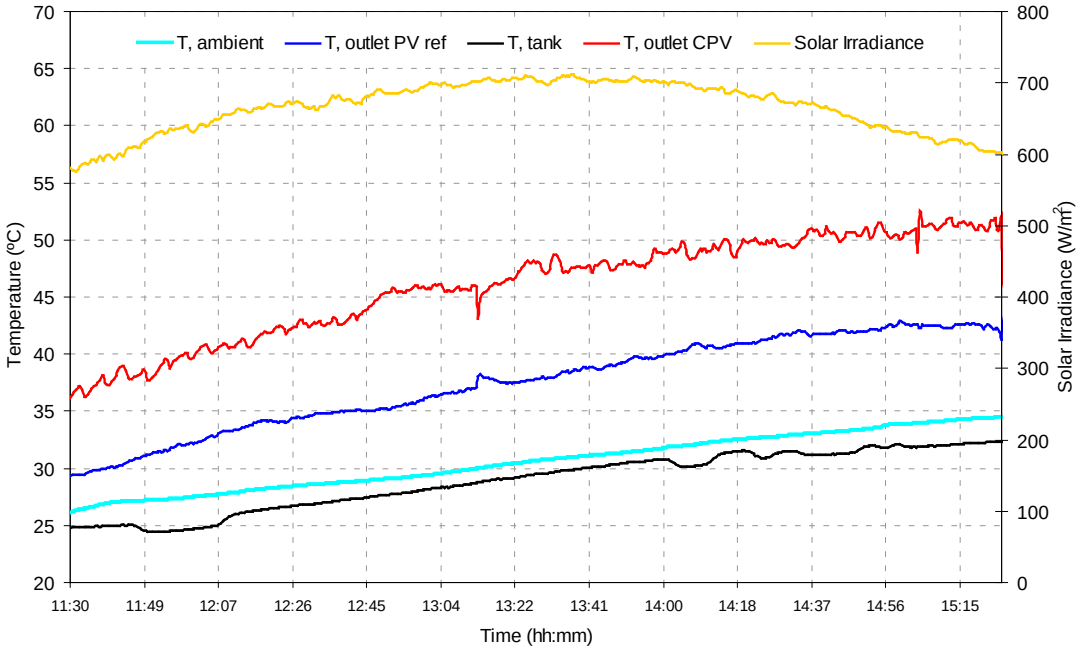

311

312 Figure 10. Temperature profiles for the reference and concentrating modules. Date:

313 26/9/2014

314

315 For a better evaluation of the joint effect of the increase of short circuit current

316 and the decrease of the open circuit potential because of the concentrated irradiance, the

317 maximum power values (P_m) are presented, considering the FF to be constant. The

318 maximum power is calculated by multiplying the short circuit current (I_{sc}), the open

319 circuit potential (V_{oc}) and the fill factor (FF), as defined in the following equation (2):

320 $$P_{mp} = I_{sc}V_{oc}FF \qquad (2)$$

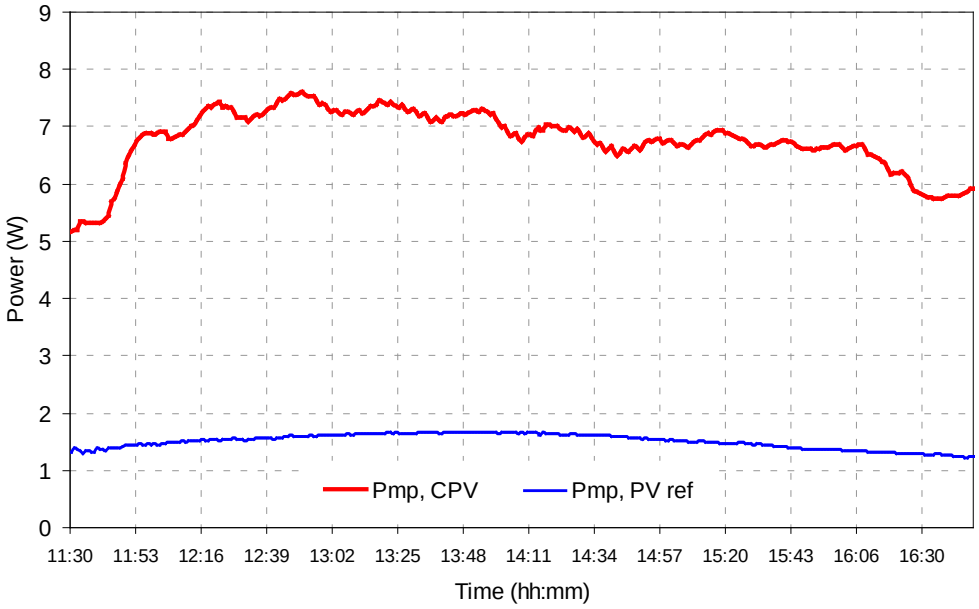

Figure 11. Maximum power output comparative profiles. Date: 26/9/2014.

From these maximum power values (Fig. 11), in order to better evaluate the differential performance, the electrical power ratio has been calculated by giving the values presented in figure 12. The electrical power ratio evaluates how many times the CPV module delivers more electrical output than the reference one. The mean electrical power takes a value of 4.51; therefore, even the decrease in voltage, the CPV module yields 4.5 times more power.

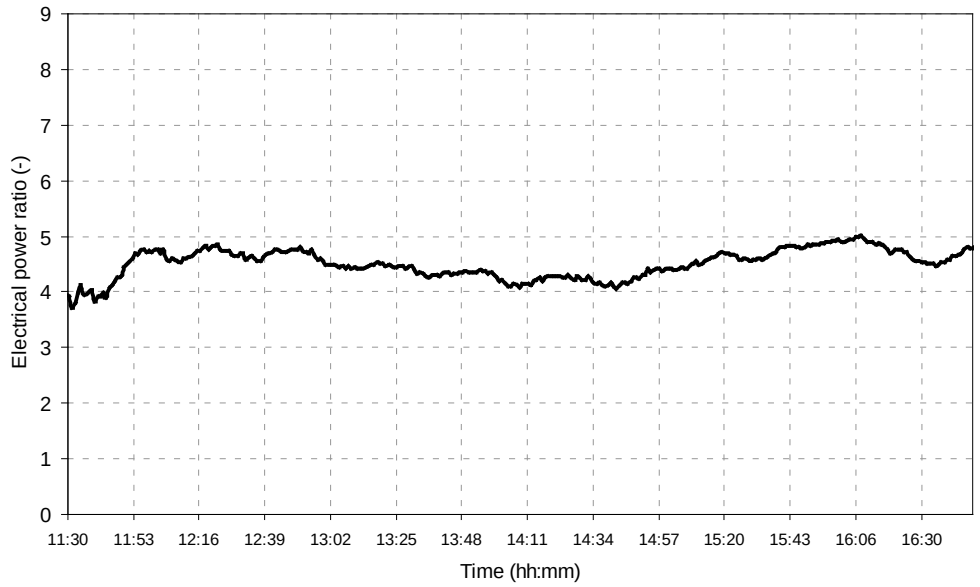

330
331 Figure 12. Electrical power ratio profile. Date: 26/9/2014.
332

333 A similar concept has been defined with respect to the thermal output, since the
334 modules are PVT. The quotient between the thermal powers produced by the two
335 modules presents the evolution charted in Figure 13. The average value obtained is
336 1.90, which means that the CPV module generates almost the double heat energy than
337 the reference one.

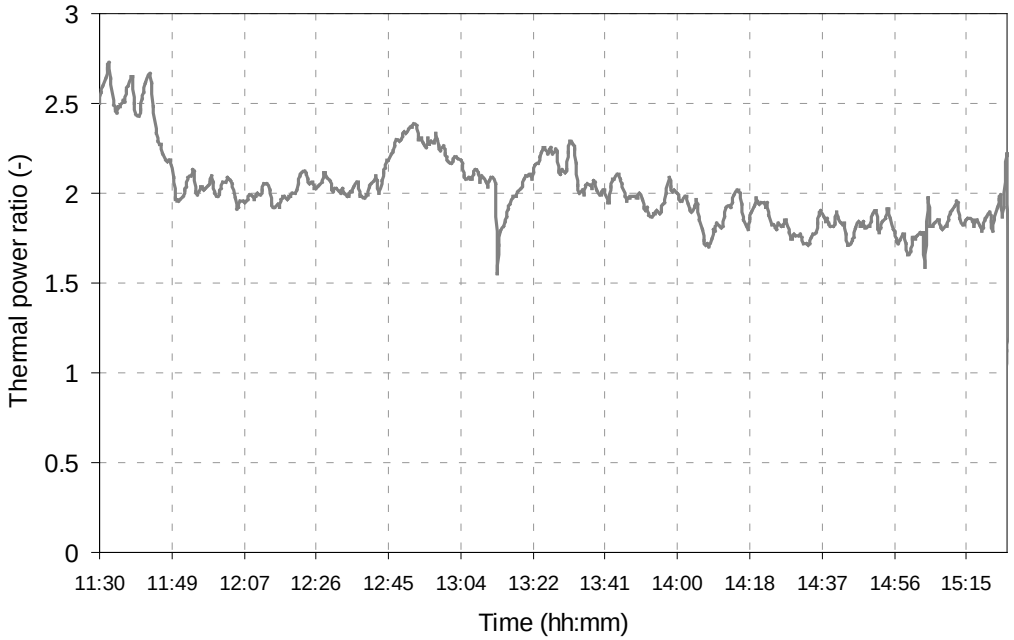

338

339 Figure 13. Thermal power ratio daily profile. Date: 26/9/2014.

In the next paragraphs, analogous results for a day with higher changes in the irradiance are included to show how the concentrating system responses to those variations. Figure 14 represents the daily evolution of the short circuit current and the open circuit voltage. It can be seen that both short circuit current profiles are in agreement with the solar irradiance one and the concentrator divergences caused by the control pulses are not bigger than in the case with a more uniform irradiance. This appreciation it can be noticed in Figure 15a, where the electrical power ratio is plotted and the average value is almost identical than that reported previously. In this case the average value is 4.68.

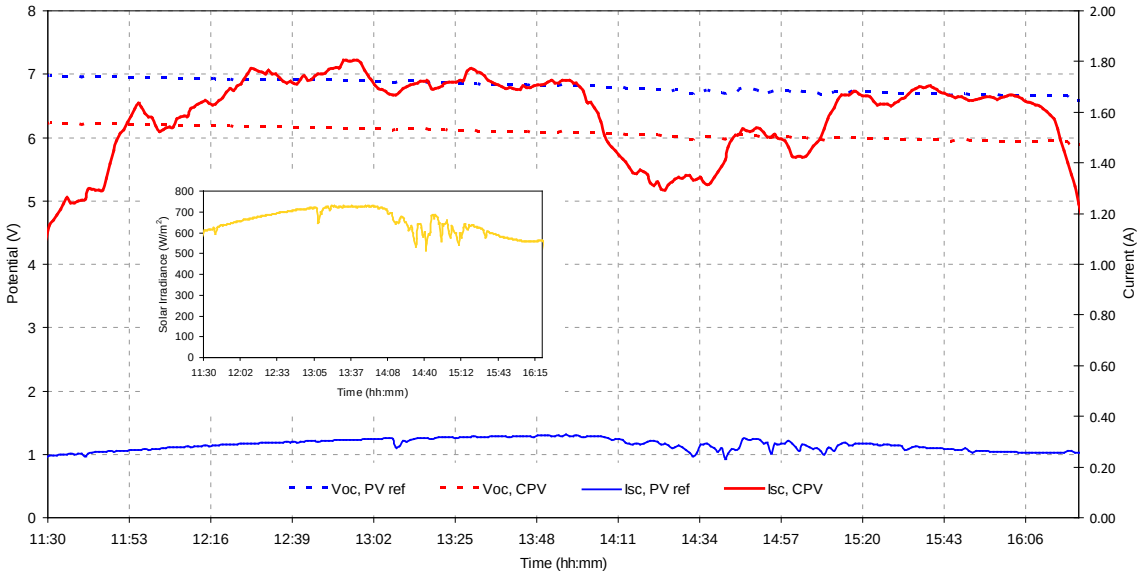

Figure 14. Irradiance, V_{oc} and I_{sc} profiles for the reference and the concentrating modules. Date: 20/9/2014.

For the case of the thermal output (Fig. 15b), the mean thermal power ratio takes a value of 2.8, which is more than 30% higher than the one obtained for the case with uniform irradiance profile. This increase can be originated because the system responses

thermally faster in the case of the concentrated irradiance achieving in proportion higher temperatures than the reference one.

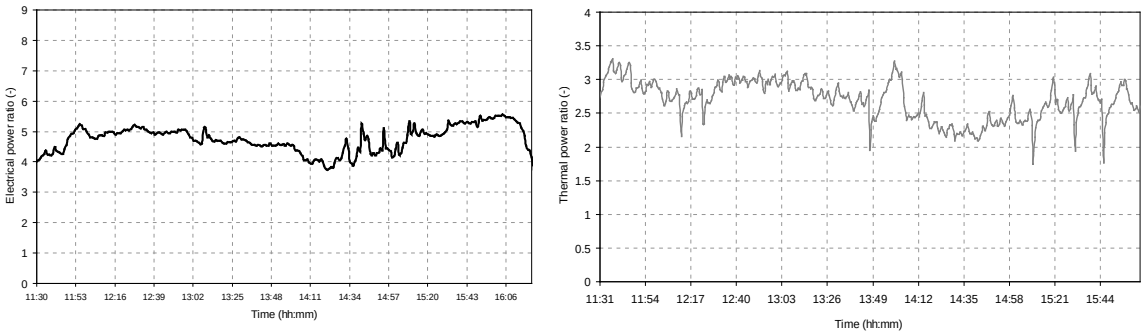

a) b)

Figure 15. a) Electrical power ratio profile; b) Thermal power ratio profile. Date: 20/9/2014.

5 Conclusions

A building façade-integrated concentrating photovoltaic-thermal system has been constructed and experimentally characterised outdoors. Every component, including concentrator, hybrid module, mechanical system and electronics, has been designed and fabricated.

The concentrator behaves achieving an average optical efficiency slightly above 51%, which is in agreement with the simulated results.

The concentrating PVT system outperforms the conventional reference PVT module in both, electrical and thermal energy production. In the case of the electrical generation the power delivered by the CPV system is about 4.5-4.7 times higher than in the reference system. For the thermal production, the thermal power ratio takes a value raging from 1.9 to 2.8 depending on the weather conditions.

The tracking system and system performance were analysed also under variable irradiance conditions to determine their sensitivity to these conditions. The tracking response was adequate as no significant decrease in the electrical power was observed due to possible tracking mismatches.

From the above commented results it can be concluded that the concentrating system presented offers advantages in energy generation which qualifies it as an attractive solution for building-integrated applications.

Acknowledgements

The authors would like to acknowledge the funding from "Ministerio de Economía y Competitividad" of Spain (grants ENE2013-48325-R and BES-2014-069596).

The authors would also like to thank networking support by the COST Action TU1205 Building Integration of Solar Thermal Systems.

References

[1] European Parliament. *Directive 2010/31/EU of the European Parliament and of the Council of 19 May 2010 on the energy performance of buildings.* 2010.

[2] Menoufi, K., Chemisana, D., Rosell, J.I. 2013, “Life cycle assessment of a building integrated concentrated photovoltaic scheme”, Appl Energy, 111, pp. 505–514.

[3] Chemisana, D. 2011, "Building integrated concentrating photovoltaics: A review", Renewable and Sustainable Energy Reviews, 15, pp. 603-611.

[4] Aste, N., Tagliabue, L.C., Del Pero, C., Testa, D., Fusco, R. 2015, “Performance analysis of a large-area luminescent solar concentrator module”, Renewable Energy, 76, pp 330-337

[5] Baig, H., Sarmah, N., Chemisana, D., Rosell, J. & Mallick, T.K. 2014, "Enhancing performance of a linear dielectric based concentrating photovoltaic system using a reflective film along the edge", Energy, 73, pp. 177-191.

[6] Baig, H., Sellami, N., Chemisana, D., Rosell, J. & Mallick, T.K. 2014, "Performance analysis of a dielectric based 3D building integrated concentrating photovoltaic system", Solar Energy, 103, pp. 525-540.

[7] Baig, H., Sellami, N. & Mallick, T.K. 2015, "Performance modeling and testing of a Building Integrated Concentrating Photovoltaic (BICPV) system", Solar Energy Materials and Solar Cells, 134, pp. 29-44.

[8] Chemisana, D., Collados, M.V., Quintanilla, M. & Atencia, J. 2013, "Holographic lenses for building integrated concentrating photovoltaics", Applied Energy, 110, pp. 227-235.

[9] Chen, R.T., Chau, J., Hwang, G.L. 2012,“Design and fabrication of diffusive solar cell window”, Renewable Energy, 40, pp. 24-28.

[10] Mallick, T.K. & Eames, P.C. 2007, "Design and fabrication of low concentrating second generation PRIDE concentrator", Solar Energy Materials and Solar Cells, 91, pp. 597-608.

[11] Sarmah, N. & Mallick, T.K. 2015, "Design, fabrication and outdoor performance analysis of a low concentrating photovoltaic system", Solar Energy, 112, pp. 361-372.

[12] Zacharopoulos, A., Eames, P.C., McLarnon, D. & Norton, B. 2000, "Linear dielectric non-imaging concentrating covers for PV integrated building facades", Solar Energy, 68, pp. 439-452.

[13] Rawlemon (2014). www. rawlemon.com., Accessed September 2014

[14] Dyson, A., Jensen, M. and Stark, P. 2007 “Integrated concentrating (IC) solar façade system”. DOE Solar Energy Technologies Program Review Meeting, April 17–19, Colorado, USA.

[15] Fthenakis, V. & Kim, H.C. 2010, "Life cycle assessment of amonix 7700 HCPV systems", AIP Conference Proceedings, pp. 260.

[16] Chemisana, D. & Ibáñez, M. 2010, "Linear Fresnel concentrators for building integrated applications", Energy Conversion and Management, 51, pp. 1476-1480.

[17] Chemisana, D. & Rosell, J.I. 2011, "Design and optical performance of a nonimaging Fresnel transmissive concentrator for building integration applications", Energy Conversion and Management, 52, pp. 3241-3248.

[18] Chemisana, D., Ibáñez, M. & Barrau, J. 2009, "Comparison of Fresnel concentrators for building integrated photovoltaics", Energy Conversion and Management, 50, pp. 1079-1084.

[19] Chemisana, D., López-Villada, J., Coronas, A., Rosell, J.I. & Lodi, C. 2013, "Building integration of concentrating systems for solar cooling applications", Applied Thermal Engineering, 50, pp. 1472-1479.

[20] Cristofari, C., Notton, G. & Canaletti, J.L. 2009, "Thermal behavior of a copolymer PV/Th solar system in low flow rate conditions", Solar Energy, 83, pp. 1123-1138.

[21] Kalogirou, S.A. & Tripanagnostopoulos, Y. 2006, "Hybrid PV/T solar systems for domestic hot water and electricity production", Energy Conversion and Management, 47, pp. 3368-3382.

[22] Buonomano, A., Calise, F., Dentice d'Accadia, M. & Vanoli, L. 2013, "A novel solar trigeneration system based on concentrating photovoltaic/thermal collectors. Part 1: Design and simulation model", Energy, 61, pp. 59-71.

[23] Lamnatou, C., Mondol, J.D., Chemisana, D. & Maurer, C. 2015, "Modelling and simulation of Building-Integrated solar thermal systems: Behaviour of the coupled building/system configuration", Renewable and Sustainable Energy Reviews, vol. 48, pp. 178-191.

[24] Lamnatou, C., Mondol, J.D., Chemisana, D. & Maurer, C. 2015, "Modelling and simulation of Building-Integrated solar thermal systems: Behaviour of the system", Renewable and Sustainable Energy Reviews, 45, pp. 36-51.

[25] Chemisana, D., Ibáñez, M., Rosell, J.I. 2011, Characterization of a photovoltaic-thermal module for Fresnel linear concentrator, Energy Conversion and Management, 52, pp. 3234–3240.

[26] Xu, G., Zhang, X., Deng, S. 2011, Experimental study on the operating characteristics of a novel low-concentrating solar photovoltaic/thermal integrated heat pump water heating system, Applied Thermal Engineering, 31, pp. 3689-3695.

[27] Aldegheri, F., Baricordi, S., Bernardoni, P., Brocato, M., Calabrese, G., Guidi, V., Mondardini, L., Pozzetti, L., Tonezzer, M., Vincenzi, D. 2014, Building integrated low concentration solar system for a self-sustainable Mediterranean villa: The Astonyshine house, Energy and Buildings, 77, pp. 355–363.

[28] Li, G., Pei, G., Ji, J., Su, Y. 2015, Outdoor overall performance of a novel air-gap-lens-walled compound parabolic concentrator (ALCPC) incorporated with photovoltaic/thermal system, Applied Energy, 144, pp. 214–223.

[29] Green, M.A. 1981, “Solar cell fill factors: General graph and empirical expressions”. Solid-State Electronics, 24, pp. 788 - 789.